Carsten Carstensen · Ronald H.W. Hoppe

Convergence analysis of an adaptive nonconforming finite element method

Abstract An adaptive nonconforming finite element method is developed and analyzed that provides an error reduction due to the refinement process and thus guarantees convergence of the nonconforming finite element approximations. The analysis is carried out for the lowest order Crouzeix-Raviart elements and leads to the linear convergence of an appropriate adaptive nonconforming finite element algorithm with respect to the number of refinement levels. Important tools in the convergence proof are a discrete local efficiency and a quasi-orthogonality property. The proof does neither require regularity of the solution nor uses duality arguments. As a consequence on the data control, no particular mesh design has to be monitored.

1 Introduction and Main Result

An adaptive finite element method (AFEM) is an efficient and reliable algorithmic tool in the numerical solution of partial differential equations. The method invokes the solution of the finite element discretized problem (SOLVE), the a posteriori error estimation of the global discretization error (ESTIMATE) by easily computable local quantities as an indication to mark selected elements (MARK) for

Supported by the DFG Research Center MATHEON "Mathematics for key technologies" in Berlin.

C. Carstensen (✉)
Department of Mathematics, Humboldt-Universität zu Berlin, Unter den Linden 6,
10099 Berlin, Germany

R.H.W. Hoppe
Institute of Mathematics, Universität Augsburg,
86159 Augsburg, Germany
Department of Mathematics, University of Houston,
Houston, TX 77204-3008, USA.

refinement, and the refinement strategy (REFINE) itself. Thus, AFEMs typically consist of successive loops of the sequence

$$\text{SOLVE} \to \text{ESTIMATE} \to \text{MARK} \to \text{REFINE}\,. \tag{1.1}$$

The development and implementation of efficient and reliable a posteriori error estimators has been the subject of intensive research in the past and has reached some level of maturity (see, e.g., the monographs [3,4,6,21,30] and the references therein). On the other hand, a rigorous convergence analysis of (1.1) relying on appropriate error reduction properties has so far only been done for conforming AFEMs [26,27] and, very recently, by the authors for a mixed finite element method (MFEM) in [17]. The main ingredients are a local discrete efficiency and a quasi-orthogonality property. The latter substitutes the Galerkin orthogonality for conforming finite element schemes and is the first main difficulty in the convergence analysis for the nonconforming finite element schemes as well. The second additional difficulty is the nonconformity in the sense that the finer discrete space V_h does not include the coarser space V_H.

This paper aims at a convergence result for a sequence of discrete fluxes computed by an adaptive nonconforming finite element method (NFEM) of the form (1.1) applied to the variational formulation of a model 2D Poisson equation with homogeneous Dirichlet boundary conditions: *Given a bounded, simply connected domain* $\Omega \subset \mathbb{R}^2$ *with polygonal boundary* $\Gamma = \partial\Omega$ *and* $f \in L^2(\Omega)$, *find* $u \in V := H^1_0(\Omega)$ *such that*

$$(\operatorname{grad} u, \operatorname{grad} v)_{0,\Omega} = (f, v)_{0,\Omega} \quad \text{for all } v \in V. \tag{1.2}$$

Here and throughout the paper $(\cdot,\cdot)_{0,\Omega}$ denotes the $L^2(\Omega)$ inner product both for square integrable functions and vector fields with square integrable components.

We discretize (1.2) by the lowest-order nonconforming P1 finite elements (Crouzeix-Raviart elements) with respect to a shape-regular triangulation $\mathcal{T}_H$ of the Lipschitz domain Ω into triangles. With the associated NFEM space $V_H := \mathrm{CR}_1(\mathcal{T}_H)$, the NFEM reads: *find* $u_H^N \in V_H$ *such that*

$$\sum_{T\in\mathcal{T}_H} (\operatorname{grad}_H u_H^N, \operatorname{grad}_H v_H^N)_{0,T} = (f, v_H^N)_{0,\Omega} \quad \text{for all } v_H^N \in V_H. \tag{1.3}$$

Here and throughout, grad_H denotes the elementwise gradient (with respect to $\mathcal{T}_H$); further details on the lowest order Crouzeix-Raviart elements are provided in Section 2; cf. also [8,11,18].

We note that efficient solvers for (1.3) such as multigrid methods and multilevel preconditioned iterative solvers have been developed, analyzed and implemented in [9,10,22,28].

The step ESTIMATE in (1.1) essentially consists of a postprocessing procedure to compute the residual-type a posteriori error estimator [15,14,19,23,24]

$$\eta := \Big(\sum_{E\in\mathcal{E}_H(\Omega)} \eta_E^2\Big)^{1/2} \quad \text{with} \quad \eta_E^2 := h_E \|[p_H^N]\|^2_{0,E}. \tag{1.4}$$

Here and throughout $\mathcal{E}_H(\Omega)$ denotes the set of interior edges and, for any such edge $E = T_+ \cap T_-$ of length h_E shared by two adjacent elements $T_\pm \in \mathcal{T}_H$, $[p_H^N]$ stands

for the jump $[p_H^N] := p_H^N|_{T_+} - p_H^N|_{T_-}$ of the discrete flux $p_H^N := \mathrm{grad}_H u_H^N$ accross E. With the unit normal and tangent vector ν_E and τ_E along $E \in \mathcal{E}_H$, the constant vector $[p_H^N]$ allows a decomposition in normal and tangential components:

$$|[p_H^N]|^2 = ([p_H^N] \cdot \nu_E)^2 + ([p_H^N] \cdot \tau_E)^2.$$

Theorem 3.5 below implies that we may omit the normal component and focus on the tangential component $[p_H^N] \cdot \tau_E =: [\partial p_H^N / \partial s]$.

Besides the edge contributions in (1.4), volume contributions play a dominant role in the adaptive algorithm below. Given the right-hand side $f \in L^2(\Omega)$ and the piecewise constant mesh-size function H, defined by $H|_T := h_T := |T|^{1/2} \approx \mathrm{diam}(T)$ on $T \in \mathcal{T}_H$, the volume contribution reads

$$\mu_H := \|H\, f\|_{0,\Omega} = \Big(\sum_{T \in \mathcal{T}_H} |T| \|f\|_{0,T}^2\Big)^{1/2}. \tag{1.5}$$

The essential role in the step MARK in (1.1) is played by refinement indicators based on the bulk criterion from [7,20,26] for displacement-based AFEMs. Given the universal constants Θ_1 with $0 < \Theta_1, \varrho_2 < 1$, the outcome of MARK is a set of edges $\mathcal{M} \subset \mathcal{E}_H$ such that

$$\Theta_1 \sum_{E \in \mathcal{E}_H} h_E \|[\partial u_H^N / \partial s]\|_{0,E}^2 \le \sum_{E \in \mathcal{M}} h_E \|[\partial u_H^N / \partial s]\|_{0,E}^2. \tag{1.6}$$

The refined regular triangulation $\mathcal{T}_h$ from REFINE generated by refining at least all the edges in $\mathcal{M}$ (and possibly further edges to avoid hanging nodes) with the new mesh-size $h \le H$ is supposed to satisfy

$$\varrho_2 \|H\, f\|_{0,\Omega}^2 \le \|h\, f\|_{0,\Omega}^2. \tag{1.7}$$

Subsection 7.1 discusses a realisation of (1.7) with a choosen Θ_2 and resulting $\varrho_2 := 1 - \Theta_2/2 < 1$. Figure 1 illustrates suitable refinements of the triangles $T \in \mathcal{T}_H$ in the step REFINE to maintain shape-regularity.

The main result of this paper is to prove the following error reduction property (1.8) for the ANFEM under consideration. Therein, u_h^N and u_H^N denote the NFEM approximations to u with respect to the triangulations $\mathcal{T}_h$ and $\mathcal{T}_H$, respectively, with flux approximations $p_h^N := \mathrm{grad}_h u_h^N$ and $p_H^N := \mathrm{grad}_H u_H^N$ to the flux $p = \mathrm{grad}\, u$.

Theorem 1.1 (error reduction property) *Under the preceding assumptions, there exist positive constants $\varrho_1 < 1$ and C_1 which depend exclusively on Θ_1 and the shape regularity of the triangulation such that*

$$\begin{pmatrix} \|p - p_h^N\|_{0,\Omega}^2 \\ \|h\, f\|_{0,\Omega}^2 \end{pmatrix} \le \begin{pmatrix} \varrho_1 & C_1 \\ 0 & \varrho_2 \end{pmatrix} \begin{pmatrix} \|p - p_H^N\|_{0,\Omega}^2 \\ \|H\, f\|_{0,\Omega}^2 \end{pmatrix}. \tag{1.8}$$

(Therein, $a \le b$ for vectors a, b means $a_j \le b_j$ for all $j = 1, 2$.)

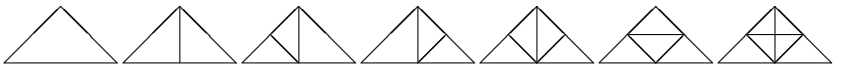

Fig. 1 Illustration of possible refinements of one triangle T in the step REFINE. Data representations and a MATLAB realization are provided in [16].

The result on one loop of (1.1) implies R-linear convergence with a reduction factor $\max\{\sqrt{\varrho_1}, \sqrt{\varrho_2}\}$ for the sequence of pairs $(\|p - p_h^N\|_{0,\Omega}, \|h\, f\|_{0,\Omega})$.

Moreover, given the parameters of (1.8), set $e_H^2 := \|p - p_H^N\|_{0,\Omega}^2 + 2C_1/(1 - \varrho_2)\|H\, f\|_{0,\Omega}^2$ and define e_h^2 correspondingly. Then, (1.8) implies the Q-linear convergence

$$e_h^2 \leq \max\{\varrho_1, (1 + \varrho_2)/2\}\, e_H^2.$$

The remaining part of this paper is organized as follows: Section 2 provides notational details and auxiliary results. The main arguments in the proof are the reliability of the estimator, a strict discrete local efficiency, and some quasi-orthogonality derived in Section 3, Section 4, and Section 5, respectively. Section 6 finalizes the proof of Theorem 1.1 on the error reduction property. A few remarks on the realization of (1.7), an example for MARK, and extensions to 3D and mixed boundary conditions plus one numerical illustration in Section 7 conclude this paper.

2 Notations and Preliminaries

2.1 General Notations

Here and in the sequel we assume that $\Omega \subset \mathbb{R}^2$ is a bounded, simply connected domain with polygonal boundary Γ. The paper adopts standard notion for Lebesgue spaces and norms. Moreover, $H(\mathrm{div}; \Omega)$ stands for the Hilbert space of vector fields $q \in L^2(\Omega)^2$ such that $\mathrm{div}\, q \in L^2(\Omega)$, equipped with the graph norm; $H(\mathrm{div}^0; \Omega) := \{q \in H(\mathrm{div}; \Omega) \mid \mathrm{div}\, q = 0\}$ refers to the subspace of solenoidal vector fields.

Throughout the rest of the paper the abbreviation $A \lesssim B$ has the meaning $A \leq C\, B$ with a mesh-size independent, generic constant $C > 0$. Moreover, $A \approx B$ abbreviates $A \lesssim B \lesssim A$.

2.2 Shape-Regular Triangulations

The domain Ω is discretized by the shape-regular simplicial triangulations $\mathcal{T}_H$ and $\mathcal{T}_h$; $\mathcal{T}_h$ is some refinement of $\mathcal{T}_H$ where each triangle T in $\mathcal{T}_H$ is refined by one of the rules of Figure 1.

A shape-regular triangulation $\mathcal{T}$ in 2D is a set of closed triangles T of positive area $|T|$ such that any two distinct triangles T_1 and T_2 are either disjoint $T_1 \cap T_2 = \emptyset$ or share exactly one vertex z, $T_1 \cap T_2 = \{z\}$, or have one edge $E = T_1 \cap T_2$ in common.

The set of vertices and edges in the triangulation $\mathcal{T}_H$ are denoted by $\mathcal{N}_H$ and $\mathcal{E}_H$, respectively. For any (closed or open) set $D \subset \overline{\Omega}$,

$$\mathcal{N}_H(D) := \mathcal{N}_H \cap D \quad \text{and} \quad \mathcal{E}_H(D) := \{E \in \mathcal{E}_H : E \subset D\}$$

denote the respective nodes and edges in D. In particular, $\mathcal{E}_H(\Omega)$ and $\mathcal{E}_H(\Gamma)$ denotes the set of interior and boundary edges in $\mathcal{T}_H$.

For $T \in \mathcal{T}_H$ with area $|T|$, define its size $h_T := |T|^{1/2} \approx \mathrm{diam}(T)$ and its center of gravity $x_T := \mathrm{mid}(T)$. For $E \in \mathcal{E}_H(T)$, recall that h_E is its lenght while

ν_E and τ_E are the unit normal and unit tangential vector. For any $E \in \mathcal{E}_H(\Omega)$ let $\omega_E := \text{int}(T_+ \cup T_-)$ (the interior of $T_+ \cup T_-$) denote its edge-patch consisting of its (at most two) neighboring triangles $T_\pm \in \mathcal{T}_H$ with $E = T_+ \cap T_-$.

The same notation with h instead of H is adopted for the fine mesh $\mathcal{T}_h$.

2.3 Data oscillations

For the fixed right-hand side $f \in L^2(\Omega)$ and any domain $D \subset \overline{\Omega}$ with area $|D| > 0$, the real number f_D denotes the integral mean of f over D, i.e.,

$$f_D := |D|^{-1} \int_D f(x)\, dx.$$

In this context, $f_H \in P_0(\mathcal{T}_H)$ and $f_h \in P_0(\mathcal{T}_h)$ denote the piecewise integral means, e.g., $f_H|_T := f_T$ for $T \in \mathcal{T}_H$.

The weighted $L^2(D)$ norm of the difference $f - f_D$ is called the oscillation of f over D and written

$$\text{osc}(f, D) := |D|^{1/2} \|f - f_D\|_{L^2(D)}.$$

In particular, given any $E \in \mathcal{E}_H(\Omega)$ and the integral mean $f_{\omega_E} := |\omega_E|^{-1} \int_{\omega_E} f(x)dx$ of f with respect to the patch ω_E, set

$$\text{osc}_E := \text{osc}(f, \omega_E) \approx h_E \|f - f_{\omega_E}\|_{0,\omega_E}$$

and $\text{osc}_H := (\sum_{E \in \mathcal{E}_H(\Omega)} \text{osc}_E^2)^{1/2}$.

A Poincaré inequality for $f \in H^1(\Omega)$ reveals that osc_H is of second order and hence of higher-order than the error terms.

2.4 Crouzeix-Raviart NFEM

The Crouzeix-Raviart NFEM space $V_H := CR_0^1(\mathcal{T}_H)$ is given by

$$\begin{aligned} \text{CR}_0^1(\mathcal{T}_H) := \{ & v_H \in L^2(\Omega) |\ \forall T \in \mathcal{T}_H,\ v_H|_T \in P_1(T); \\ & \forall E \in \mathcal{E}_H(\Omega),\ v_H \text{ is continuous at } \text{mid}(E); \\ & \forall E \in \mathcal{E}_H(\Gamma),\ v_H(\text{mid}(E)) = 0\}. \end{aligned}$$

Here and throughout $P_k(T)$, $k \geq 0$, denotes the linear space of polynomials of degree $\leq k$ on $T \in \mathcal{T}_H$. The solution $u_H^N \in V_H := \text{CR}_0^1(\mathcal{T}_H)$ of (1.3) is called the Crouzeix-Raviart NFEM approximation of $u \in H_0^1(\Omega)$, and the elementwise gradients $p_H^N := \text{grad}_H u_H^N$ are referred to as the discrete fluxes.

The edge-oriented basis functions of V_H are denoted by $(\psi_E : E \in \mathcal{E}_H(\Omega))$, i.e., given any $E \in \mathcal{E}_H(\Omega)$ the function ψ_E is defined by $\psi_E(\text{mid}(E)) = 1$ and $\psi_E(\text{mid}(F)) = 0$ for any other edge $F \in \mathcal{E}_H$.

Algorithms and data structures as well as documented MATLAB implementations are given in [5].

A discrete Poincaré inequality for nonconforming functions concludes this subsection on Crouzeix-Raviart NFEM.

Lemma 2.1 *Given some fixed $T \in \mathcal{T}_H$ let $\mathcal{T}_h(T)$ denote the triangulation of T with respect to the fine mesh as illustrated in Figure 1. Let $V_T := \mathrm{CR}^1_0(\mathcal{T}_h(T))$ denote the Crouzeix-Raviart NFEM space (without boundary conditions) on T. Then, there holds*

$$\min_{w\in\mathbb{R}} \|w_h - w\|_{0,T} \approx h_T \, \|grad_h w_h\|_{0,T} \quad \text{for all } w_h \in V_T.$$

Proof The left and right-hand side of the assertion define norms on the finite-dimensional vector space $V_T/\mathbb{R}$ (e.g., the subspace of functions in V_T with integral mean zero). Since those norms are equivalent, there holds the claimed equivalence. A transformation argument to the reference triangle proves that, for each of the finite configurations of Figure 1, the equivalence constants do not depend on the mesh-size and solely depends on the minimum angle in the triangle T. □

2.5 Raviart-Thomas MFEM

The Raviart-Thomas MFEM space $\mathrm{RT}_0(\Omega;\mathcal{T}_H)$ and the linear space of element-wise constants $P_0(\mathcal{T}_H)$ are given by

$$\begin{aligned}\mathrm{RT}_0(\mathcal{T}_H) := \{q_H \in H(\mathrm{div},\Omega) \,|\forall T \in \mathcal{T}_H \,\exists a \in \mathbb{R}^2 \,\exists b \in \mathbb{R} \,\forall x \in T,\\ q_H(x) = a + bx\},\\ P_0(\mathcal{T}_H) := \{v_H \in L^\infty(\Omega) \,|\forall T \in \mathcal{T}_H,\ \ v_H|_T \in P_0(T)\}\,.\end{aligned}$$

The MFEM approximation of (1.2) amounts to the computation of $u_H^M \in P_0(\mathcal{T}_H)$ and $p_H^M \in \mathrm{RT}_0(\mathcal{T}_H)$ such that for all $q_H \in \mathrm{RT}_0(\mathcal{T}_H)$ and $v_H \in P_0(\mathcal{T}_H)$ there holds [12]

$$(p_H^M, q_H)_{0,\Omega} \,+\, (u_H^M, \mathrm{div}\, q_H)_{0,\Omega} = 0\,, \tag{2.1}$$

$$(\mathrm{div}\, p_H^M, v_H)_{0,\Omega} = -\,(f_H, v_H)_{0,\Omega}\,. \tag{2.2}$$

The spaces $\mathrm{CR}^1_0(\mathcal{T}_h)$, $\mathrm{RT}_0(\mathcal{T}_h)$, and $P_0(\mathcal{T}_h)$ as well as the NFEM and MFEM approximations u_h^N, p_h^N and u_h^M, p_h^M are defined analogously.

2.6 Equivalence of Crouzeix-Raviart and Raviart-Thomas FEM

The discrete fluxes p_H^N and p_H^M defined by the respective Crouzeix-Raviart and Raviart-Thomas FEM are related.

Lemma 2.2 ([5,25]) *For $T \in \mathcal{T}_H$ recall $f_T := \int_T f(x)\,dx/|T|$ and $x_T :=$ mid(T). Then there holds*

$$p_H^N|_T(x) = \, p_H^M(x)|_T \,+\, \frac{1}{2}\, f_T(x - x_T) \quad \text{for all } x \in T \in \mathcal{T}_H. \quad \square \tag{2.3}$$

An immediate consequence of Lemma 2.2 (given without further proof) concludes this subsection.

Lemma 2.3 *There holds $\|p_H^N - p_H^M\|_{0,\Omega} \lesssim \|H\, f\|_{0,\Omega}$.* □

3 Reliable error estimators

The reliability of error estimators for NFEM approximations has been studied in [1,2,13–15,19,23,24,29].

Those works established the following theorem stated in the notation of the previous sections.

Theorem 3.1 ([19]) *There holds* $\|p - p_H^N\|_{0,\Omega} \lesssim \eta + \|H\, f\|_{0,\Omega}$. □

A refined version thereof appeared in [13–15] where the volume term $\|H\, f\|_{0,\Omega}$ is substituted by edge contributions plus oscillations.

Theorem 3.2 ([13]) *There holds* $\|p - p_H^N\|_{0,\Omega} \lesssim \eta + \mathrm{osc}_H$. □

A new proof of Theorem 3.2 is based on the following identity.

Lemma 3.3 *Given any interior edge* $E \in \mathcal{E}_H(\Omega)$*, let* $\psi_E \in \mathrm{CR}_0^1(\mathcal{T}_H)$ *be the edge-basis function with supp* $\psi_E \subset \overline{\omega_E}$*. Then there holds*

$$[p_H^N] \cdot \nu_E \;=\; h_E^{-1}\,(f, \psi_E)_{0,\omega_E}. \tag{3.1}$$

Proof Since $[p_H^N] \cdot \nu_E \in P_0(E) \equiv \mathbb{R}$, we have

$$h_E\,[p_H^N] \cdot \nu_E \;=\; ([p_H^N], \nu_E)_{0,E} = ([p_H^N] \cdot \nu_E, \psi_E)_{0,E}.$$

Since ψ_E is L^2-orthogonal onto constants on all edges except E, since $\mathrm{div}_H\, p_H^N = 0$ and since ψ_E is an admissible test function for the NFEM with support in $\overline{\omega_E}$, the application of Green's formula yields

$$\begin{aligned}([p_H^N] \cdot \nu_E, \psi_E)_{0,E} &= ([p_H^N] \cdot \nu_E, \psi_E)_{0,E} + ([p_H^N] \cdot \nu_E, \psi_E)_{0,\partial\omega_E} \\ &= (p_H^N, \mathrm{grad}_H\, \psi_E)_{0,\omega_E} + (\mathrm{div}_H\, p_H^N, \psi_E)_{0,\omega_E} \\ &= (f, \psi_E)_{0,\omega_E}.\end{aligned}$$

□

An immediate consequence of (3.1) is the following result.

Lemma 3.4 *There holds*

$$h_E\,\|f\|_{0,\omega_E} \approx \Big(\sum_{E \in \mathcal{E}_H(\Omega)} h_E \|[p_H^N] \cdot \nu_E\|_{0,E}^2\Big)^{1/2} \pm \mathrm{osc}_E \tag{3.2}$$

in the sense that $h_E\|f\|_{0,\omega_E} \lesssim h_E^{1/2}\|[p_H^N] \cdot \nu_E\|_{0,E} + \mathrm{osc}_E$ *and* $h_E^{1/2}\|[p_H^N] \cdot \nu_E\|_{0,E} \lesssim h_E\|f\|_{0,\omega_E} + \mathrm{osc}_E$.

Proof Lemma 3.3 and $\int_{\omega_E} \psi_E dx = |\omega_E|/3$ show

$$\begin{aligned}h_E\,\|f_{\omega_E}\|_{0,\omega_E} &\lesssim |\omega_E|\,|f_{\omega_E}| \\ &= 3\,|(f_{\omega_E}, \psi_E)_{0,\omega_E}| \\ &\le 3\,|(f_{\omega_E} - f, \psi_E)_{0,\omega_E}| + 3\,|(f, \psi_E)_{\omega_E}| \\ &\lesssim h_E\,\|f - f_{\omega_E}\|_{0,\omega_E} + h_E^{1/2}\|[p_H^N] \cdot \nu_E\|_{0,E}.\end{aligned}$$

This proves one assertion of the lemma. Its converse follows by the same arguments. □

The announced new proof of Theorem 3.2 simply replaces the volume contribution $\|H\,f\|_{0,\Omega}$ in Theorem 3.1 by its upper bound

$$\left(\sum_{E\in\mathcal{E}_H(\Omega)} h_E^2\|f\|_{0,\omega_E}^2\right)^{1/2} \lesssim \left(\sum_{E\in\mathcal{E}_H(\Omega)} h_E\|[p_H^N]\cdot\nu_E\|_{0,E}^2\right)^{1/2} + \operatorname{osc}_H\,.$$

This argument can be used also to replace the normal components in the right-hand side of Theorem 3.1. In this way, one deduces the following reliability result the authors have not found in the literature.

Theorem 3.5 (Reliability) *There holds*

$$\|p-p_H^N\|_{0,\Omega} \lesssim \Big(\sum_{E\in\mathcal{E}_H(\Omega)} h_E\|[\partial u_H/\partial s]\|_{0,E}^2\Big)^{1/2} + \|H\,f\|_{0,\Omega}. \qquad \square$$

4 Discrete Local Efficiency

This section provides the first of two main arguments for error reduction. Unlike for conforming AFEM, there is no further restriction in REFINE throughout this paper.

Theorem 4.1 (Strict discrete local efficiency) *Suppose that $E=\partial T_+\cap\partial T_-\in\mathcal{E}_H$ is an edge in $\mathcal{T}_H$ [shared by the triangles $T_+, T_-\in\mathcal{T}_H$] which is bisected in the refinement, i.e., $E=E_1\cup E_2\notin\mathcal{E}_h$ and* $\operatorname{mid}(E)=E_1\cap E_2\in\mathcal{N}_h$ *for two distinct $E_1, E_2\in\mathcal{E}_h$. Then there holds*

$$h_E^{1/2}\|[\partial u_H^N/\partial s]\|_{0,E} \lesssim \|p_h^N - p_H^N\|_{0,\omega_E}. \tag{4.1}$$

Proof Let φ_E be a multiple of the conforming P_1 FEM basis function with respect to the nodal point $\operatorname{mid}(E)$ such that $\varphi_E(\operatorname{mid}(E)) = h_E[p_H^N]\cdot\tau_E$. Notice that

$$\|\vec{\operatorname{curl}}\,\varphi_E\|_{0,\omega_E}^2 \lesssim h_E\,\|[p_H^N]\cdot\tau_E\|_{0,E}^2. \tag{4.2}$$

Stokes' theorem shows

$$\frac{1}{2}h_E\|[\partial u_H/\partial s]\|_{0,E}^2 = (\varphi_E, [p_H^N]\cdot\tau_E)_{0,E} = (\vec{\operatorname{curl}}\varphi_E, p_H^N)_{0,\omega_E}.$$

Since $\partial\varphi_E/\partial s$ is constant along any edge F of the refined triangulation $\mathcal{T}_h$ and since $[u_h^N]$ has vanishing integral mean along F, all integrals of $[u_h^N]\partial\varphi_E/\partial s$ over F vanish. This, an integration by parts, and $\operatorname{div}_h\vec{\operatorname{curl}}\,\varphi_E = 0$ yield

$$(\vec{\operatorname{curl}}\varphi_E, p_h^N)_{0,\omega_E} = ([u_h^N], \partial\varphi_E/\partial s)_{0,E} = 0.$$

The two preceding identities imply

$$\begin{aligned}\frac{1}{2}\,h_E\,\|[p_H^N]\cdot\tau_E\|_{0,E}^2 &= (\vec{\operatorname{curl}}\,\varphi_E, p_H^N - p_h^N)_{\omega_E}\\ &\le \|\vec{\operatorname{curl}}\,\varphi_E\|_{0,\omega_E}\,\|p_h^N - p_H^N\|_{0,\omega_E}.\end{aligned}$$

The combination of this with (4.2) proves (4.1). $\square$

5 Quasi-Orthogonality

The second main argument for error reduction is a generalization of the Galerkin orthogonality in the conforming AFEM [20,26,27].

Theorem 5.1 (Quasi-orthogonality) *There holds*

$$|(p - p_h^N, p_H^N - p_h^N)_{0,\Omega}| \lesssim \|H\, f\|_{0,\Omega} \left(\|p - p_h^N\|_{0,\Omega} + \|p - p_H^N\|_{0,\Omega} \right). \quad (5.1)$$

The rest of this section is devoted to the proof of Theorem 5.1. The left-hand side in the assertion (5.1) is split as

$$\begin{aligned}(p - p_h^N, p_H^N - p_h^N)_{0,\Omega} &= (p - p_h^N, p_H^M - p_h^M)_{0,\Omega} \\ &\quad + (p - p_h^N, (p_H^N - p_H^M) - (p_h^N - p_h^M))_{0,\Omega}. \quad (5.2)\end{aligned}$$

Lemma 2.3 can be applied to estimate the L^2 norm of $p_H^N - p_H^M$ on the coarse mesh as well as that of $p_h^N - p_H^h$ on the fine mesh with the same upper bound $\lesssim \|H\, f\|_{0,\Omega}$. This and (5.2) lead to

$$\begin{aligned}(p - p_h^N, p_H^N - p_h^N)_{0,\Omega} &\lesssim (p - p_h^N, p_H^M - p_h^M)_{0,\Omega} \\ &\quad + \|H\, f\|_{0,\Omega} \|p - p_h^N\|_{0,\Omega}. \quad (5.3)\end{aligned}$$

An elementwise application of Green's formula is followed by $-\mathrm{div}\, p_h^M = f_h$ and $-\mathrm{div}\, p_H^M = f_H$ and the observation that emerging boundary integrals vanish because $(p_H^M - p_h^M) \cdot \nu_E$ is constant along $E \in \mathcal{E}_h(\Omega)$ and $\int_E [u - u_h^N] ds = \int_E [u_h^N] ds = 0$. Hence,

$$\begin{aligned}(p - p_h^N, p_h^M - p_h^M)_{0,\Omega} &= \sum_{T \in \mathcal{T}_h} (p - p_h^N, p_H^M - p_h^M)_{0,T} \\ &= \sum_{E \in \mathcal{E}_h(\Omega)} ([u - u_h^N], (p_H^M - p_h^M) \cdot \nu_E)_{0,E} \\ &\quad + \sum_{T \in \mathcal{T}_h} (u - u_h^N, f_H - f_h)_{0,T} \\ &= (u - u_h^N, f_H - f_h)_{0,\Omega}. \quad (5.4)\end{aligned}$$

It is essential to observe that on each $T \in \mathcal{T}_H$, the piecewise constant $f_H - f_h$ has integral mean zero. Hence an elementwise Poincaré inequality for $e := u - u_H^N \in H^1(T)$ with integral mean $e_T \in \mathbb{R}$ shows

$$\begin{aligned}(u - u_H^N, f_H - f_h)_{0,T} &= (e - e_T, f_H - f_h)_{0,T} \\ &\leq h_T/\pi \|\mathrm{grad}_H e\|_{0,T} \|f_H - f_h\|_{0,T}.\end{aligned}$$

Lemma 2.1 allows a corresponding argument for $(u_H^N - u_h^N, f_H - f_h)_{0,T}$ and $w_h := u_H^N - u_h^N$ and $w := (w_h)_T \in \mathbb{R}$ leads to

$$\begin{aligned}(w_h, f_H - f_h)_{0,T} &= (w_h - w, f_H - f_h)_{0,T} \\ &\lesssim h_T \|\mathrm{grad}_h w_h\|_{0,T} \|f_H - f_h\|_{0,T}.\end{aligned}$$

The combination of the preceding two inequalities and their sum over all triangles in $T \in \mathcal{T}_H$ shows (after further triangle inequalities)

$$(u - u_h^N, f_H - f_h)_{0,\Omega} \lesssim \|Hf\|_{0,T}(\|p - p_h^N\|_{0,\Omega} + \|p - p_H^N\|_{0,\Omega}). \quad (5.5)$$

The combination of (5.3)–(5.5) concludes the proof of (5.1). □

6 Error Reduction

This section is devoted to the proof of Theorem 1.1 and combines the reliability estimate, the bulk criterion, the discrete local efficiency and the quasi-orthogonality.

The first argument is the reliability from Theorem 3.5, namely

$$\|p - p_H^N\|_{0,\Omega} \lesssim \Big(\sum_{E\in\mathcal{E}_H(\Omega)} h_E\|[\partial u_H^N/\partial s]\|_{0,E}^2\Big)^{1/2} + \|H\,f\|_{0,\Omega}. \quad (6.1)$$

A reformulation with the bulk criterion (1.6) and the set of refined edges $\mathcal{M}$ reads

$$\sum_{E\in\mathcal{E}_H(\Omega)} h_E\|[\partial u_H^N/\partial s]\|_{0,E}^2 \lesssim \sum_{E\in\mathcal{M}} h_E\|[\partial u_H^N/\partial s]\|_{0,E}^2. \quad (6.2)$$

Since at least all $E \in \mathcal{M}$ are refined, the discrete efficiency estimate of Theorem 4.1 leads to the upper bound (4.1). The sum of all such estimates leads to

$$\sum_{E\in\mathcal{M}} h_E\|[\partial u_H^N/\partial s]\|_{0,E}^2 \lesssim \sum_{E\in\mathcal{M}} \|p_h^N - p_H^N\|_{0,\omega_E}^2 \lesssim \|p_h^N - p_H^N\|_{0,\Omega}^2. \quad (6.3)$$

The quasi-orthogonality of Theorem 5.1 shows

$$\begin{aligned}\|p_h^N - p_H^N\|_{0,\Omega}^2 + \|p - p_h^N\|_{0,\Omega}^2 - \|p - p_H^N\|_{0,\Omega}^2 &= -2(p - p_h^N, p_h^N - p_H^N)_{0,\Omega}\\ &\lesssim \|Hf\|_{0,\Omega}(\|p - p_h^N\|_{0,\Omega} + \|p - p_H^N\|_{0,\Omega}). \quad (6.4)\end{aligned}$$

In the combination of (6.1)–(6.4), there is some positive constant $\kappa < 1/2$ independent of h, H such that

$$\begin{aligned}3\kappa\,\|p - p_H^N\|_{0,\Omega}^2 \le \|p - p_H^N\|_{0,\Omega}^2 - \|p - p_h^N\|_{0,\Omega}^2 + \|H\,f\|_{0,\Omega}^2\\ +\|Hf\|_{0,\Omega}(\|p - p_h^N\|_{0,\Omega} + \|p - p_H^N\|_{0,\Omega}). \quad (6.5)\end{aligned}$$

Two Young's inequalities for the last term in (6.5) lead to

$$\begin{aligned}\|Hf\|_{0,\Omega}(\|p - p_h^N\|_{0,\Omega} + \|p - p_H^N\|_{0,\Omega}) \le (2\kappa)^{-1}\|Hf\|_{0,\Omega}^2 + \kappa\|p - p_h^N\|_{0,\Omega}^2\\ +\kappa\|p - p_H^N\|_{0,\Omega}^2. \quad (6.6)\end{aligned}$$

The combination of (6.5)-(6.6) shows the claimed estimate

$$\|p - p_h^N\|_{0,\Omega}^2 \le \varrho_1\,\|p - p_H^N\|_{0,\Omega}^2 + C\,\|Hf\|_{0,\Omega}^2 \quad (6.7)$$

of Theorem 1.1 with $\varrho_1 := (1-2\kappa)/(1-\kappa) < 1$ and $C_1 := (1+(2\kappa)^{-1})/(1-\kappa)$ $\lesssim 1$. □

7 Remarks

The notation and technicalities were kept minimal throughout this work. Some comments on algorithms and extentions conclude this paper.

7.1 Data Reduction

Since the Crouzeix-Raviart NCFEM is edge-oriented, the following edge-oriented quantities are involved with equivalent weights. For each edge $E \in \mathcal{E}_H(\Omega)$ (with respect to the coarse triangulation $\mathcal{T}_H$) set

$$\mu_{H,E}^2 := \frac{|T_+|}{m_+} \|f\|_{0,T_+}^2 + \frac{|T_-|}{m_-} \|f\|_{0,T_-}^2 \tag{7.1}$$

where $E = T_+ \cap T_-$ for the two neighboring triangles $T_\pm \in \mathcal{T}_H$ with integers $m_\pm := \mathrm{card}(\mathcal{E}_H(\Omega) \cap \mathcal{E}_H(T_\pm))$. (The number $m_\pm \geq 1$ counts the number of interior edges amongst the edges of the element $T_\pm$ and hence, the multiplicity of the contribution in the sum over all edges in $\mathcal{E}_H(\Omega)$.) In this way we have

$$\mu_H^2 := \sum_{E \in \mathcal{E}_H(\Omega)} \mu_{H,E}^2 = \sum_{T \in \mathcal{T}_H} |T| \, \|f\|_{0,T}^2 = \|H\, f\|_{0,\Omega}^2.$$

With a new parameter Θ_2 with $0 < \Theta_2 < 1$, the data reduction (1.7) is realized by

$$\Theta_2 \sum_{E \in \mathcal{E}_H(\Omega)} \mu_{H,E}^2 \leq \mu_H^2 := \sum_{E \in \mathcal{M}} \mu_{H,E}^2. \tag{7.2}$$

Lemma 7.1 *Suppose* (7.2) *and that (at least) any edge in* $\mathcal{M}$ *is refined in* $\mathcal{T}_h$. *Then there holds* (1.7) *with* $\varrho_2 := (1 - \Theta_2/2) < 1$.

Proof Consider one triangle $K \in \mathcal{T}_h$ which is contained in some $T \in \mathcal{T}_H$ with $\mathcal{E}_H(T) \cap \mathcal{M} \neq \emptyset$. Then $K \subset T$ is at least halved and hence $|K| \leq |T|/2$. As a consequence,

$$\mu_h^2 \leq 1/2 \sum_{E \in \mathcal{M}} \mu_{H,E}^2 + \sum_{E \in \mathcal{E}_H(\Omega) \setminus \mathcal{M}} \mu_{H,E}^2 = \mu_H^2 - 1/2 \sum_{E \in \mathcal{M}} \mu_{H,E}^2.$$

With μ_H and (7.2) this reads

$$\Theta_2/2\, \mu_H^2 \leq 1/2 \sum_{E \in \mathcal{M}} \mu_{H,E}^2 \leq \mu_H^2 - \mu_h^2. \qquad \square$$

7.2 Algorithm MARK

This subsection is devoted to the realization of the step MARK in each loop (1.1) of an adaptive algorithm to ensure (1.6)-(1.7): *Given* $\eta_{H,E}^2 := h_E \|[\partial u_H^N / \partial s]\|_{0,E}^2$ *and* $\mu_{H,E}$ *(from* (7.1)*) for any* $E \in \mathcal{E}_H(\Omega)$ *initiate* $\mathcal{M}_0 := \emptyset$ *and* $k = 0$.

(a) If $\Theta_1 \sum_{E\in\mathcal{E}_H(\Omega)} \eta_{H,E}^2 \le \sum_{E\in\mathcal{M}_k} \eta_{H,E}^2$ *go to (b) else select some* $F \in \mathcal{E}_H(\Omega) \setminus \mathcal{M}_k$ *with*

$$\eta_{H,F} = \max_{G\in\mathcal{E}_H(\Omega)\setminus\mathcal{M}_k} \eta_{H,G}$$

and set $\mathcal{M}_{k+1} := \mathcal{M}_k \cup \{F\}$ *and* $k := k+1$.

(b) If $\Theta_2 \sum_{E\in\mathcal{E}_H(\Omega)} \mu_{H,G}^2 \le \sum_{E\in\mathcal{M}_k} \mu_{H,E}^2$ *go to (c) else select some* $F \in \mathcal{E}_H(\Omega) \setminus \mathcal{M}_k$ *with*

$$\mu_{H,F} = \max_{G\in\mathcal{E}_H(\Omega)\setminus\mathcal{M}_k} \mu_{H,G}$$

and set $\mathcal{M}_{k+1} := \mathcal{M}_k \cup \{F\}$ *and* $k := k+1$.

(c) Given $\mathcal{M}_k$ *mark further edges to obtain the output* $\mathcal{M}$ *with the closure property to avoid hanging nodes while maintaining the shape regularity in the refinements indicated in Figure 1.*

Output the set of marked edges $\mathcal{M}$:=*MARK*$(\mathcal{E}_H(\Omega))$.

7.3 Extension to 3D

Throughout the paper, Theorem 1.1 has been proven in a 2D setting for notational simplicity. This subsection discusses the 3D version of Theorem 1.1 and outlines the small modifications in its proof.

The changes in the notation from 2D to 3D are well established and hence not repeated here; for instance, the edges E are replaced by faces and the Helmholtz decomposition in 3D involves different notations of the curl and of the trace to replace $[\partial u_H^N/\partial s]$. Details can be found in [15] along with a proof of Theorem 3.2 in 3D. Lemma 3.4 holds verbatim in 3D and so does Theorem 3.5.

One crucial detail in the 3D version of Theorem 4.1 is that the refined face E does require an inner node mid(E) such that ϕ_E can be designed as in the proof of Theorem 4.1. The remaining details on vanishing surface integrals and integration by parts can be adopted from [15], in particular from Theorem 3.2 therein.

A proof of the 3D version of Lemma 2.2 is included in [5] and hence Theorem 5.1 follows as well. The remaining details are immediate and hence omitted.

7.4 Mixed Boundary Conditions

The Laplace equation with homogeneous Dirichlet boundary conditions serves as a model example in this paper for the ease of this discussion. A general mixed boundary value problem would involve the approximation errors of the Dirichlet data u_D and the Neumann data g. The explicit terms in the reliable and efficient error estimation (an extended version of Theorem 3.2) are derived in [14] and are shown to contain $\eta_E^2 := h_E \int_E |g - \partial u_H^N/\partial s|^2 ds$ for edges $E \subset \Gamma_N$ as well as data oscillations. This requires to treat corresponding data terms in g and u_D plus the displayed volume terms with f in a data reduction step (1.7). The technicalities in the extended proofs are straightforward and hence omitted.

7.5 Numerical Experiment

The mixed boundary value problem on the L-shaped domain $\Omega = (-1, 1) \times (0, 1) \cup (-1, 0) \times (-1, 0]$ with Dirichlet boundary $\Gamma_D = [0, 1] \times \{0\} \cup \{0\} \times [-1, 0]$ and Neumann boundary $\Gamma_N := \partial\Omega \setminus \Gamma_D$,

$$\begin{aligned} -\Delta u &= 0 \text{ in } \Omega, \\ u &= 0 \text{ on } \Gamma_D, \\ \partial u/\partial n &= g \text{ on } \Gamma_N \end{aligned}$$

allows for an exact solution $u(r, \varphi) = r^{2/3} \sin(2\varphi/3)$ in polar coordinates where the smooth Neumann data g is computed from that. Figure 3 shows the meshes generated by the adaptive algorithm with MARK from Subsection 7.2 (with η_E for $E \subset \Gamma_N$). The meshes refine towards the re-entering corner at $(0, 0)$ where the exact solution has a generic singularity. Notice that the bulk-criterion, in general, leads to non-symmetric refinement visible in Figure 3.

Figure 2 shows the energy error norm and its approximation via the error estimator as functions of the number of degrees of freedom N. The experimental convergence rates support the optimal convergence $\propto N^{-1/2}$) for the adaptive algorithm compared to a sub-optimal convergence $\propto N^{-1/3}$ for uniform mesh refinements.

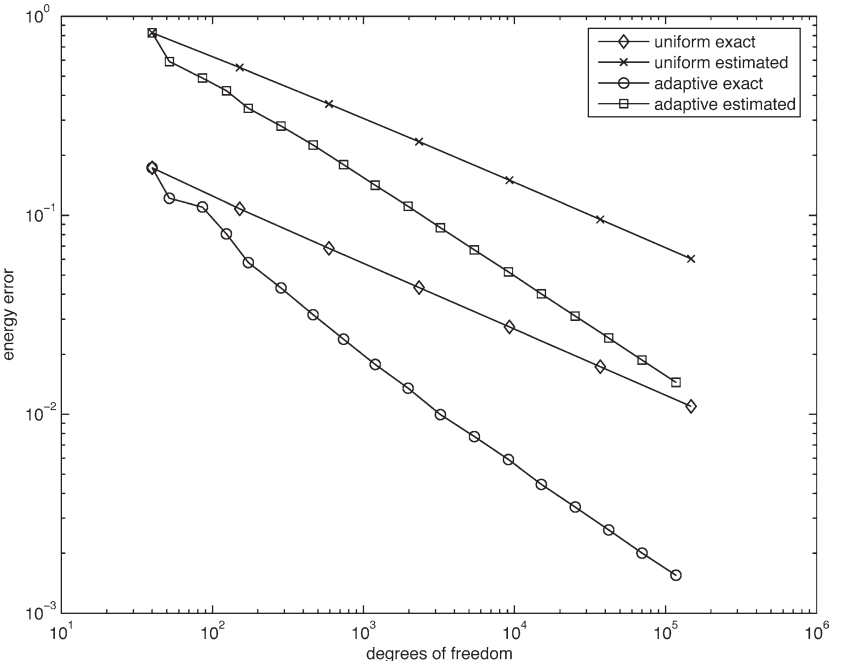

Fig. 2 Energy Error Norm and Error Estimator Plotted as a Function of the Degrees of Freedom for Uniform and Adaptive Mesh Refinements.

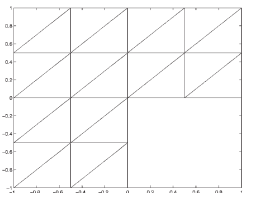

(a) $\mathcal{T}_0$

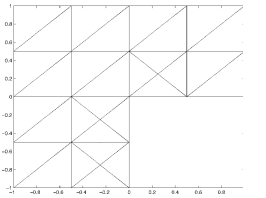

(b) $\mathcal{T}_1$

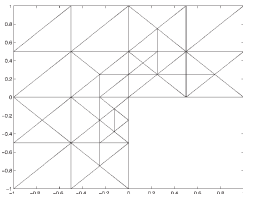

(c) $\mathcal{T}_2$

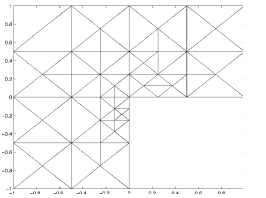

(d) $\mathcal{T}_3$

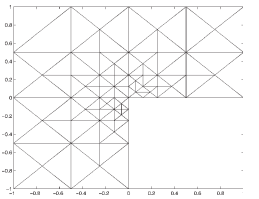

(e) $\mathcal{T}_4$

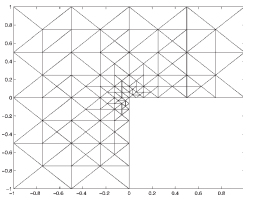

(f) $\mathcal{T}_5$

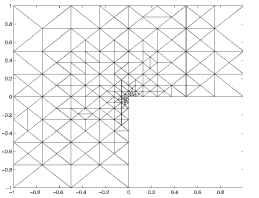

(g) $\mathcal{T}_6$

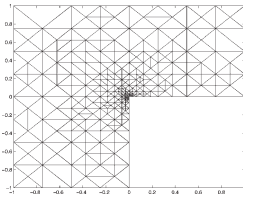

(h) $\mathcal{T}_7$

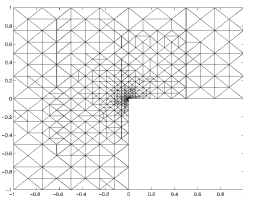

(i) $\mathcal{T}_8$

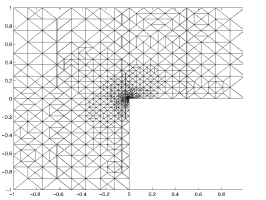

(j) $\mathcal{T}_9$

Fig. 3 Triangulations $\mathcal{T}_0, \ldots, \mathcal{T}_9$ of L-shaped Domain Ω Generated by the Adaptive Algorithm Based on MARK from Subsection 7.2.

Acknowledgements The authors thank David Günther and Jan Reininghaus for providing the numerical example of Figure 2 and 3.

The work of the first author (CC) was supported by the Austrian Science Fund (FWF) under Project P15274 and P16461 and the German Research Association (DFG) within the DFG Research Center "Mathematics for key technologies" Project C13. The work of the second author was partially suported by the National Science Foundation under Grant No. DMS-0411403 and Grant No. DMS-0412267.

References

1. Agouzal, A.: A posteriori error estimator for nonconforming finite element methods. Appl. Math. Lett. **7**, 1017–1033 (1994)
2. Ainsworth, M.: Robust a posteriori error estimation for non-conforming finite element approximation. SIAM J Numer. Anal. **42** (2005) no 6, 2320–2341.
3. Ainsworth, M., Oden, J.T.: A posteriori error estimation in finite element analysis. Wiley, Chichester, 2000
4. Babuska, I., Strouboulis, T.: The finite element method and its reliability. Clarendon Press, Oxford, 2001
5. Bahriawati, C., Carstensen, C.: Three Matlab implementations of the lowest-order Raviart-Thomas MFEM with a posteriori error control. Computational Methods in Applied Mathematics, Vol 5 (2005) No 4, 333–361
6. Bangerth, W., Rannacher, R.: Adaptive finite element methods for differential equations. Lectures in Mathematics. ETH-Zürich. Birkhäuser, Basel, 2003
7. Binev, P., Dahmen, W., DeVore, R.: Adaptive finite element methods with convergence rates. Numer. Math. **97**, 219–268 (2004)
8. Braess, D.: Finite elements. Cambridge University Press, Cambridge, 1997
9. Braess, D., Verfürth, R.: Multigrid methods for nonconforming finite element methods. SIAM J. Numer. Anal. **27**, 979–986 (1990)
10. Brenner, S.: An optimal order multigrid method for nonconforming finite elements. Math. Comp. **52**, 1–15 (1989)
11. Brenner, S., Scott, L.R.: The mathematical theoty of finite element methods. Springer, New York, 1994
12. Brezzi, F., Fortin, M.: Mixed and hybrid finite element methods. Springer, Berlin-Heidelberg-New York, 1991
13. Carstensen, C.: Quasi-interpolation and a posteriori error analysis in finite element method. M2AN **33**, 1187–1202 (1999)
14. Carstensen, C., Bartels, S.: Each averaging technique yields reliable a posteriori error control in FEM on unstructured grids. I. Low order conforming, nonconforming and mixed FEM. Math. Comp. **71**(239), 945–969 (2002)
15. Carstensen, C., Bartels, S., Jansche, S.: A posteriori error estimates for nonconforming finite element methods. Numer. Math. **92**, 233–256 (2002)
16. Carstensen, C., Bolte, J.: Adaptive mesh-refining algorithm for courant finite elements in matlab. data structures and algorithms. (2006) (in preparation)
17. Carstensen, C., Hoppe, R.H.W.: Error reduction and convergence for an adaptive mixed finite element method. To appear in Math. Comp. (2006)
18. Ciarlet, P.G.: The finite element method for elliptic problems. Nort-Holland, Amsterdam, 1978
19. Dari, E., Duran, R., Padra, C., Vampa, V.: A posteriori error estimators for nonconforming finite element methods. RAIRO Model. Math. Anal. Numer. **30**, 385–400 (1996)
20. Dörfler, W.: A convergent adaptive algorithm for Poisson's equation. SIAM J. Numer. Anal. **33**(3), 1106–1124 (1996)
21. Eriksson, K., Estep, D., Hansbo, P., Johnson, C.: Computational differential equations. Cambridge University Press, Cambridge, 1995
22. Hoppe, R.H.W., Wohlmuth, B.: Adaptive multilevel iterative techniques for nonconforming finite element discretizations. East-West J. Numer. Math. **3**, 179–197 (1995)
23. Hoppe, R.H.W., Wohlmuth, B.: Element-oriented and edge-oriented local error estimators for nonconforming finite element methods. RAIRO Model. Math. Anal. Numer **30**, 237–263 (1996)

24. Kanschat, G., Suttmeier, F.-T.: A posteriori error estimates for nonconforming finite element schemes. Calcolo **36**, 129–141 (1999)
25. Marini, L.D.: An inexpensive method for the evaluation of the solution of the lowest order Raviart-Thomas mixed method. SIAM J. Numer. Anal. **22**(3), 493–496 (1985)
26. Morin, P., Nochetto, R.H., Siebert, K.G.: Data oscillation and convergence of adaptive FEM. SIAM J. Numer. Anal. **38**(2), 466–488 (2000)
27. Morin, P., Nochetto, R.H., Siebert, K.G.: Local problems on stars: a posteriori error estimators, convergence, and performance. Math. Comp. **72**(243), 1067–1097 (2003)
28. Oswald, P.: On a hierarchical basis multilevel method with nonconforming P1 elements. Numer. Math. **62**, 189–212 (1992)
29. Schieweck, F.: A posteriori error estimates with post-processing for nonconforming finite elements. ESAIM Math. Mod. Numer. Anal. **36**, 489–503 (2002)
30. Verfürth, R.: A review of a posteriori error estimation and adaptive mesh-refinement techniques. Wiley-Teubner, New York, Stuttgart, 1996